

Supporting Material

Effect of sphingomyelin head group size on molecular properties and interactions with cholesterol

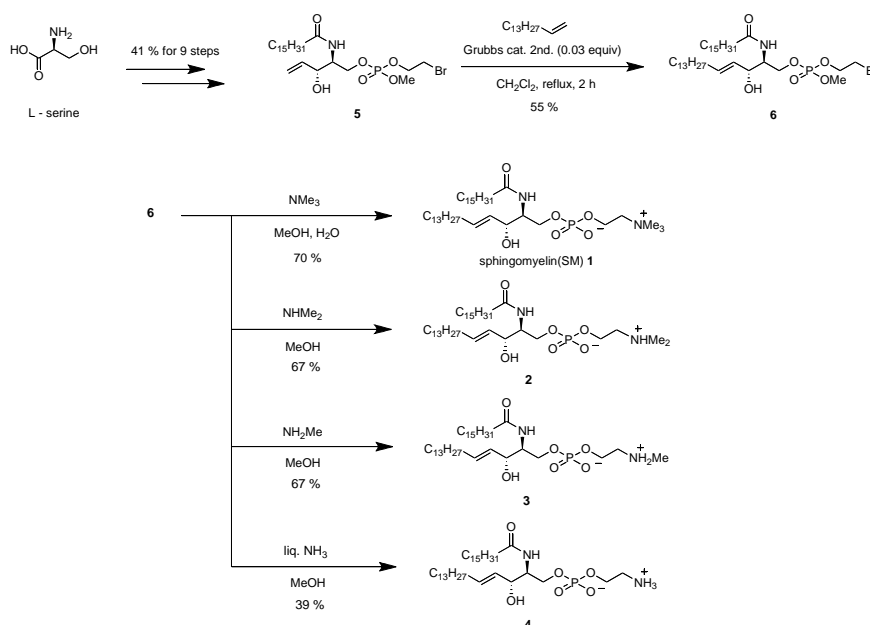
Anders Björkbom, Tomasz Róg, Karol Kaszuba, Mayuko Kurita, Shou Yamaguchi, Max Lönnfors, Thomas K.M. Nyholm, Ilpo Vattulainen, Shigeo Katsumura, and J. Peter Slotte

Synthesis of SM analogs.....	1
Commercial chemicals and experimental procedures.....	3
Analysis of Atomistic MD simulations.....	5
TABLE S1 Partial charges at the choline, intermediate groups and amine.....	6
Fig. S2 DSC.....	6
Fig. S3 <i>t</i>Pa anisotropy.....	7
Fig. S4 Order parameter profiles.....	7
Fig. S5 Density profiles.....	8
Fig. S6 Snapshot of CPE-Me and CPE-Me₂.....	8
References.....	9

Synthesis of SM analogs

We designed an amino alcohol (**6** in Fig. S1) as an effective synthetic precursor for the amine derivatives of the SM choline moiety. The amino alcohol (**6**) was synthesized by an olefin cross metathesis coupling reaction between (**5**) and 1-pentadecene. Substrate (**5**) was prepared from L-serine in a 9 step reaction (41% yield) according to (1). Treatment of (**6**) with dimethylamine in methanol produced CPE-Me₂ (**2**) (67% yield), treatment with methylamine in methanol produced CPE-Me (**3**) (67% yield) and treatment with liquid ammonia produced CPE (**4**) (39% yield). The SM analogs were purified with preparative reverse phase HPLC (Supelco Discovery C-18 column, 25 cm × 21.2 mm, 5 μm particle size) with the following eluants CPE-Me₂ (methanol/H₂O, (99:1, by vol)), CPE-Me₂ (methanol) and CPE (methanol/H₂O, (96:4, by vol)). The purity and identity of the SM analogs was controlled using analytical reverse-phase HPLC (Supelco Discovery C-18 column, 25 cm × 4.6 mm, 5 μm particle size) and mass spectrometry (Ultra Performance High Capacity Ion Trap MS with electrospray ionization, Bruker Daltonics, Bremen, Germany). The SM analogs were dissolved as follows: CPE (methanol/mQ-H₂O, 9:1 by vol), CPE-Me (methanol), CPE-Me₂ (methanol) and PSM (hexane/2-propanol, 2:3 by vol).

Figure S1. Synthesis scheme



Synthesis of CPE-Me₂ (**2**)

Dimethylamine (1.0 ml) was added to a solution of **6** (0.10 g, 0.136 mmol) in methanol (1.0 ml) in a sealed tube at room temperature. The reaction mixture was stirred for 12 h at the same temperature followed by concentration in vacuo to give the crude products. Column chromatography on silica gel (from 10 % methanol in chloroform to 3 % water and 27 % methanol in chloroform) gave **2** (0.063 g, 67 %) as a colorless solid.

$[\alpha]_D^{20} +6.71$ (c 0.41, CHCl_3); IR (KBr disk, cm^{-1}) 3275, 3021, 2955, 2919, 2851, 2399, 2347, 1628, 1468; ^1H NMR (400 MHz, CD_3OD) δ 5.70 (dt, $J=14.88, 6.64\text{Hz}$, 1H), 5.44 (dt, $J=7.56, 7.56\text{Hz}$, 1H), 4.19-3.87 (m, 6H), 3.37 (dt, $J=5.27, 5.27\text{Hz}$, 2H), 2.93 (s, 6H), 2.20-2.16 (m, 2H), 2.05-2.00 (m, 2H), 1.64-1.48 (bm, 2H), 1.48-1.23 (m, 46H), 0.90 (t, $J=6.64\text{Hz}$, 6H); ^{13}C NMR (CD_3OD , 100 MHz) δ 175.9, 135.2, 131.2, 72.5, 66.0 (d, $J_{\text{CP}} = 5.8\text{Hz}$), 60.4 (d, $J_{\text{CP}} = 5.8\text{Hz}$), 59.2 (d, $J_{\text{CP}} = 7.7\text{Hz}$), 55.2 (d, $J_{\text{CP}} = 6.7\text{Hz}$), 43.6, 37.4, 35.4, 33.5, 33.1, 30.88, 30.84, 30.81, 30.79, 30.71, 30.65, 30.51, 30.49, 30.47, 30.42, 27.2, 23.8, 14.5; ESI-HRMS m/z calcd for $\text{C}_{38}\text{H}_{77}\text{N}_2\text{O}_6\text{P}$ ($\text{M}+\text{Na}$) $^+$ 711.5417, found 711.5449

Synthesis of CPE-Me (3)

Methylamine (1.0 ml) was added to solution of **6** (0.097 g, 0.132 mmol) in methanol (1.0 ml) in a sealed tube at room temperature. The reaction mixture was stirred for 12 h at the same temperature followed by concentration in vacuo to give the crude products. Column chromatography on silica gel (from 10 % methanol in chloroform to 3 % water and 27 % methanol in chloroform) gave **3** (0.059 g, 67 %) as a colorless solid.

$[\alpha]_D^{20} +8.34$ (c 0.38, CHCl_3); IR (KBr disk, cm^{-1}) 3245, 2955, 2917, 2849, 2486, 1655, 1637, 1461, 1253; ^1H NMR (400 MHz, CD_3OD) δ ; 6.47 (b, 1H), 5.68 (dt, $J=14.42, 6.64\text{Hz}$, 1H), 5.46 (dt, $J=6.64\text{Hz}$, 2H), 5.14-4.90 (b, 1H), 4.30-3.81 (m, 6H), 3.19-3.07 (b, 2H), 2.68 (s, 3H), 2.13 (t, $J=7.10\text{Hz}$, 2H), 1.98 (dt, $J=6.87, 6.87\text{Hz}$, 2H), 1.62-1.49 (b, 2H), 1.49-1.16 (m, 46H), 0.87 (t, $J=6.41\text{Hz}$, 6H); ^{13}C NMR (CD_3OD , 100 MHz) δ 176.0, 135.1, 131.1, 72.7, 66.0 (d, $J_{\text{CP}}=6.1\text{Hz}$), 61.6 (d, $J_{\text{CP}}=4.8\text{Hz}$), 55.4 (d, $J_{\text{CP}}=6.7\text{Hz}$), 51.0 (d, $J_{\text{CP}}=6.7\text{Hz}$), 37.4, 33.6, 33.4, 33.0, 30.77, 30.73, 30.69, 30.68, 30.66, 30.62, 30.53, 30.46, 30.37, 27.1, 23.6, 14.4; ESI-HRMS m/z calcd for $\text{C}_{37}\text{H}_{75}\text{N}_2\text{O}_6\text{P}$ ($\text{M}+\text{Na}$) $^+$ 697.5260, found 697.5269

Synthesis of CPE (4)

Liquid ammonia (5.0 ml) was added to a solution of **6** (0.050 g, 0.068 mmol) in methanol (5.0 ml) in a sealed tube at room temperature. The reaction mixture was stirred for 12 h at the same temperature followed by concentration in vacuo to give the crude products. Column chromatography on silica gel (from 10 % methanol in chloroform to 3 % water and 27 % methanol in chloroform) gave **4** (0.017 g, 39 %) as a colorless solid.

$[\alpha]_D^{20} +8.91$ (c 0.23, CHCl_3); IR (KBr disk, cm^{-1}): 3213, 2455, 2217, 1635, 1187; ^1H NMR (400 MHz, CD_3OD) δ ; 5.71 (dt, $J = 6.64, 14.19\text{Hz}$, 1H), 5.461 (dt, $J = 7.32, 7.32\text{Hz}$, 1H), 4.16-3.91, (m, 6H), 3.18-3.15 (m, 2H), 2.21-2.17 (m, 2H), 2.06-2.01 (m, 2H), 1.65-1.53 (m, 2H), 1.44-1.25 (m, 46H), 0.902 (t, $J = 7.10\text{Hz}$); ^{13}C NMR (CD_3OD , 100 MHz) δ 175.9, 135.0, 131.1, 72.7, 65.9 (d, $J_{\text{CP}}=4.8\text{Hz}$), 62.8 (d, $J_{\text{CP}}=2.9\text{Hz}$), 55.4 (d, $J_{\text{CP}}=6.7$), 41.8 (d, $J_{\text{CP}}=6.7\text{Hz}$), 37.4, 33.4, 33.0, 30.78, 30.77, 30.65, 30.57, 30.48, 30.42, 27.1, 23.7, 14.4; ESI-HRMS m/z calcd for $\text{C}_{36}\text{H}_{73}\text{N}_2\text{O}_6\text{P}$ ($\text{M}+\text{Na}$) $^+$ 683.5104, found 683.5104

Commercial chemicals and experimental procedures

Cholesterol, methyl- β -cyclodextrin (m β CD) and 1,2-dipalmitoyl-*sn*-glycero-3-phosphoethanolamine (DPPE) were from Sigma (St Louis, MO, USA). 1,6-Diphenyl-3,5-hexatriene (DPH) was from Molecular Probes (Eugene, OR, USA) and *trans*-parinaric acid (*t*Pa) from Cayman Chemical Company (Ann Arbor, MI, USA). 1,2-Dipalmitoyl-*sn*-glycero-3-phosphoethanolamine-N-methyl (DPPE-Me), 1,2-dipalmitoyl-*sn*-glycero-3-phosphoethanolamine-N,N-dimethyl (DPPE-Me₂), 1,2-dipalmitoyl-*sn*-glycero-3-phosphocholine (DPPC) and 1-palmitoyl-2-oleoyl-*sn*-glycero-3-phosphocholine (POPC) were from Avanti Polar Lipids (Alabaster, AL, USA). Commercial lipids were of very high purity and used without further purification. The lipids were dissolved as follows: DPPE (methanol/chloroform, 1:4 by vol), DPPE-Me (methanol/chloroform, 3:2 by vol), DPPE-Me₂ (methanol/chloroform, 3:2 by vol), DPPC (hexane/2-propanol, 2:3 by vol) and POPC (hexane/2-propanol, 2:3 by vol). Cholesta-5,7,9(11)-trien-3-beta-ol (CTL) was synthesized according to (2) and purified as described in (3). PSM was purified from egg yolk sphingomyelin (Avanti Polar Lipids) as described in (4). 1-Palmitoyl-2-stearoyl-(7-doxyl)-*sn*-glycero-3-phosphocholine (7SLPC) was synthesized and purified as described in (3) (and references within). The purity and identity of CTL and 7SLPC were confirmed using mass spectrometry (Ultra Performance High Capacity Ion Trap MS with electrospray or atmospheric pressure chemical ionization (Bruker Daltonics, Bremen, Germany)). DPH, CTL, *t*Pa and 7SLPC were stored in an argon environment at -87°C in the dark. Before use CTL and DPH were dissolved in argon purged ethanol, *t*Pa in argon purged methanol and 7SLPC in argon purged hexane/2-propanol, (2:3, by vol) and used within 3 days. All solvents used were of at least HPLC grade purity. Stock solutions of all lipids were stored at -20°C in the dark and warmed to ambient temperature before use. The H₂O used for phosphate-buffer preparation was purified with a Millipore UF Plus purification system, giving a product with an 18.2 M Ω cm resistivity. The 10 mM phosphate-buffer (pH 7.4) contained 140 mM NaCl and 0.1 mM EDTA.

Vesicle preparation

Vesicles were prepared by mixing appropriate lipid and probe solutions followed by solvent evaporation (N₂ at ~40°C). The lipid/probe mixture was then redissolved in a neat solvent (dichloromethane) followed by solvent evaporation (N₂ at ~40°C) and drying in vacuum (30 minutes at room temperature). Preheated phosphate buffer was added to the lipid film and the suspension was hydrated for 20 minutes above T_m of the highest melting lipid. The lipid-buffer suspension was briefly vortexed and either probe sonicated (Branson probe sonifier W-450, 25% duty cycle, power output 10 W, Branson Ultrasonics, Danbury, CT, USA) for 2 min to form multilamellar vesicles (MLVs) or bath sonicated (Branson bath sonicator 2510, Branson Ultrasonics) followed by the extrusion procedure (Avanti mini extruder using 0.2 μ m polycarbonate membranes filter, (Avanti Polar Lipids, Alabaster, AL, USA)) to form large unilamellar vesicles. The size distribution of large unilamellar vesicles was controlled with a Malvern Zetasizer Nano-S (Malvern Instruments Ltd, Worcestershire, UK). Extrusion and sonication were performed at temperatures exceeding T_m of the highest melting lipid and samples were protected from light during all experimental steps.

Fluorescence spectroscopy

All fluorimetric experiments were performed on T-state Quanta Master spectrofluorimeters (Photon Technology International, Lawrenceville, NJ, USA). Fluorescence quenching of Cholesta-5,7,9(11)-trien-3-beta-ol (CTL) by 1-palmitoyl-2-stearoyl-(7-doxyl)-*sn*-glycero-3-phosphocholine (7SLPC) followed the assay thoroughly described in (5). Measurements were

performed with emission and excitation slits set to 5 nm using a 50 μ M MLV solution. The F₀-sample was composed of 1-palmitoyl-2-oleoyl-*sn*-glycero-3-phosphocholine (POPC)/head group analog/cholesterol/CTL (60:30:9:1, molar ratio) and in the F-sample 7SLPC replaced 50 mol% of POPC. The temperature was increased at 5°C/min (constant stirring) and CTL was excited at 324nm and emission measured at 374 nm.

Steady-state fluorescence anisotropy measurements were performed with excitation and emission slits set to 5 nm for 1,6-diphenyl-3,5-hexatriene (DPH) and to 5 nm and 10 nm for *t*Pa. Samples were either composed of a single lipid and 1 mol% DPH (50 μ M MLV solution) for T_m measurements or POPC/head group analog/cholesterol (60:30:10, molar ratio) and 1 mol% *t*Pa (100 μ M MLV solution prepared through bath sonication for 10 min above T_m) for measurement of ordered domain melting. For DPH and *t*Pa the excitation and emission wavelengths were 360/430 nm and 305/410 nm respectively and the temperature was increased at 5°C/min (constant stirring). The anisotropy was calculated as described in (6).

Sterol partitioning assay

The partitioning of CTL between large unilamellar vesicles and methyl- β -cyclodextrin (m β CD) was measured and calculated as described in (7). Vesicles were composed of POPC/head group analog, (8:2 molar ratio) and measurements were performed at 23°C and 37°C. The results are displayed as the molar fraction partition coefficient (K_x) of CTL versus head group size for SM and PC analogs.

Atomistic MD simulations

Atomic-scale MD simulations were performed for single-component and two-component membrane systems for all SM analogs (8 systems in total). The single-component membranes were composed of 128 lipids, and the two-component bilayers of 128 lipids together with 32 cholesterol molecules (20 mol% cholesterol). All bilayers were hydrated with approximately 3600 water molecules. The initial structures of all membranes were obtained from SM and SM-cholesterol bilayers previously simulated for 100 ns at higher temperature (unpublished data). The simulations were performed using the GROMACS software package (8, 9) over 100 ns, where the first 20 ns were considered as an equilibration period (10) and the remaining 80 ns of the trajectory was analyzed.

To parameterize the interactions for lipid molecules in the systems, we used the all-atom OPLS (optimized potentials for liquid simulation) force field (11). Partial charges in the PC head groups were not originally included in the OPLS set and were taken from (12). This set of charges was derived in compliance with the OPLS methodology. For CPE-Me₂ and CPE-Me, the partial charges for the head groups were not present in the OPLS parameter set or available elsewhere, thus we calculated them by fitting the electrostatic potential of a given molecule using the restrained electrostatic potential method (13). The electronic structure and the electrostatic potential were calculated with the 6-31G* basis set, compatible with the OPLS force field, using the GAUSSIAN software suite for electronic structure calculations (14). The charges used in the modified fragments are given in Table S1. For water, we employed the TIP3P model which is compatible with the OPLS parameterization (15).

The simulation setup used in this study is identical to our previous simulation of lipid bilayers with the OPLS-AA parameterization (16, 17). Periodic boundary conditions with the usual minimum image convention were used in all three directions. The LINCS algorithm (18) was used to preserve hydrogen covalent bond lengths. The time step was set to 2 fs and the simulations were carried out at constant pressure (1 bar) and temperature (343 K). The temperature and pressure were controlled by the Nose-Hoover thermostat and Parrinello-Rahman barostat (19-21) using time constants of 0.2 and 2 ps, in respective order. The temperatures of the solute and solvent were controlled independently. For pressure, we used a

semi-isotropic control. The Lennard-Jones interactions were cut off at 1.0 nm, and for the electrostatic interactions we employed the particle mesh Ewald method (22) with a real space cutoff of 1.0 nm, β -spline interpolation (order of 6), and direct sum tolerance of 10^{-6} .

Analysis of atomistic simulations

To characterize structural properties of the lipid bilayers, we calculated the average area per lipid. In one-component systems, the area can be uniquely defined as the total membrane area divided by the number of lipids in a single leaflet. For many-component membranes the situation is more complicated as there is no straightforward way to calculate the area per individual lipid species (23). In this work, we calculated the average area per phospholipid by first subtracting the contribution of cholesterol from the total membrane area and then dividing the remaining area by the number of phospholipids in a leaflet. To this end, we assumed the area per cholesterol to be 0.39 nm^2 in all systems (24); earlier atomistic simulations of fluid-like DPPC-cholesterol bilayers have shown that the cross-sectional area of cholesterol is essentially constant for cholesterol concentrations up to 40 mol% (10). To describe the ordering of hydrocarbon chains, we computed the deuterium order parameter (S_{CD}) profiles along the chains using Eq. 1

$$S_{CD} = \left\langle \frac{3}{2} (\cos^2 \theta) - \frac{1}{2} \right\rangle \quad [1]$$

where θ is the angle between the C-D bond and the bilayer normal, and the brackets $\langle \rangle$ denote averaging over time and all phospholipids (25). To estimate membrane thickness we calculated the P-P distance (the distance between the average positions of phosphorus atoms in the opposite leaflets). The average tilt of the cholesterol ring (with respect to membrane normal direction) was defined through the vector linking atoms C3 in ring A and C17 in ring D.

At the water-membrane interface the molecules interact via strong non-bonded interactions, that is, H-bonds and charge pairs. Charge pairs are characteristic especially to phosphatidylcholine head groups in terms of electrostatic interactions between the positively charged choline methyl groups and the negatively charged oxygen atoms (26). The presence of H-bonds was evaluated on the basis of geometrical criteria derived in our previous studies: the distance between donor and acceptor is less than or equal to 0.325 nm, and the angle between the vector linking donor and acceptor and the vector given by the chemical bond between hydrogen and donor is less than or equal to 35° (27-29). To determine the existence of charge groups we used a distance cutoff of 0.4 nm (26).

TABLE S1 Partial charges at the choline, intermediate groups and amine

Atom	Me ₃	Me ₂	Me ₁	Me ₀
HN	-	0.25	0.27	0.34
C _{Me}	-0.34	-0.23	-0.16	-
H _{Me}	0.17	0.17	0.16	-
N	0.33	-0.10	-0.10	-0.33
C4	-0.02	0.11	0.02	0.05
H4	0.09	0.11	0.11	0.11

Partial charges at the choline, intermediate groups and amine of the SM analogs. HN is the hydrogen attached directly to nitrogen, C_{Me} is the carbon of the methyl group, H_{Me} the hydrogen attached to C_{Me}, N the nitrogen, C4 is the carbon of the methylene group, and H4 is the hydrogen attached to C4.

Figure S2. Melting of gel phase as observed with DSC on systems composed of POPC/SM-analog (2:1, molar ratio). Lipid dispersions (1.4 mM) were prepared with bath sonication and the graphs shown are heating scans (1.0°C/min). Experiments were performed on a Microcal VP-DSC (GE Healthcare) and accompanying software. Note: PSM formed a thermogram with two peaks but incubation of vesicles above T_m decreased the duality of the peak. The displayed PSM data is from vesicles incubated above T_m.

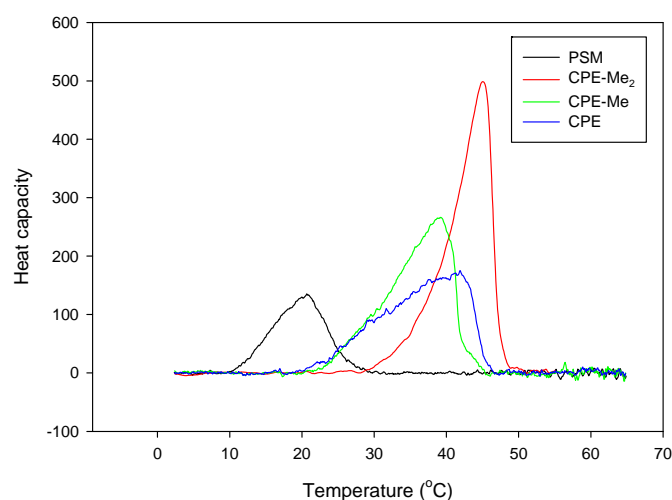


Figure S3. Melting of gel domains for SM analogs in an otherwise fluid lipid matrix as measured with the anisotropy of tPa . Melting of gel domains is shown as a function of head group size according to PSM (*black*), CPE-Me₂ (*red*), CPE-Me (*green*) and CPE (*blue*). Samples consisted of POPC/SM analog (2:1 molar ratio) and experiments were performed as described in the methods section.

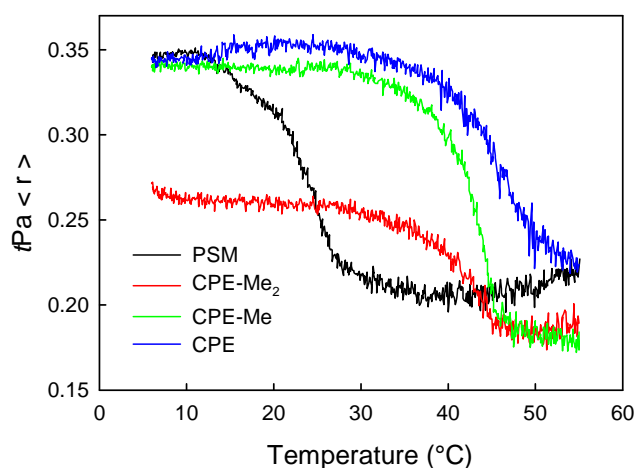


Figure S4. Profiles of the order parameter S_{CD} for the sphingosine tail (A), and the acyl tail (B). The small segment numbers correspond to the region close to the head group.

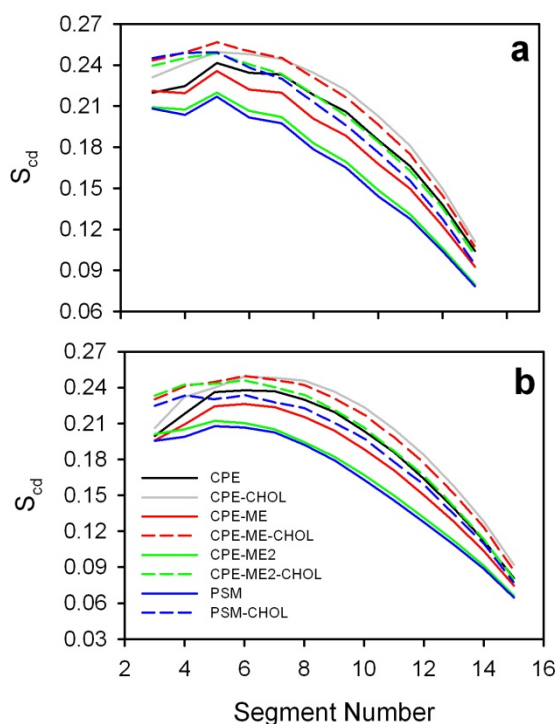


Figure S5. Density profiles of the selected polar groups in the CPE-Me bilayer. Membrane depth of 0 nm corresponds to membrane centre.

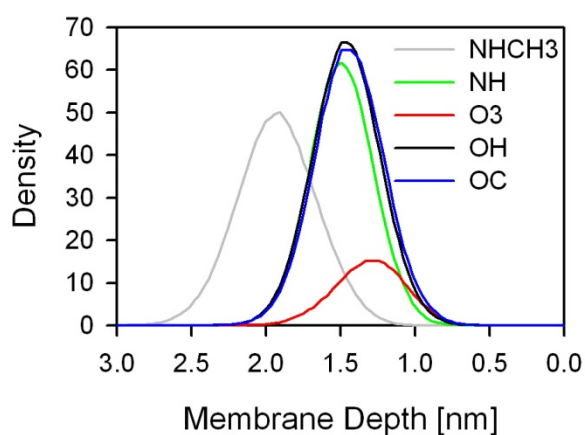
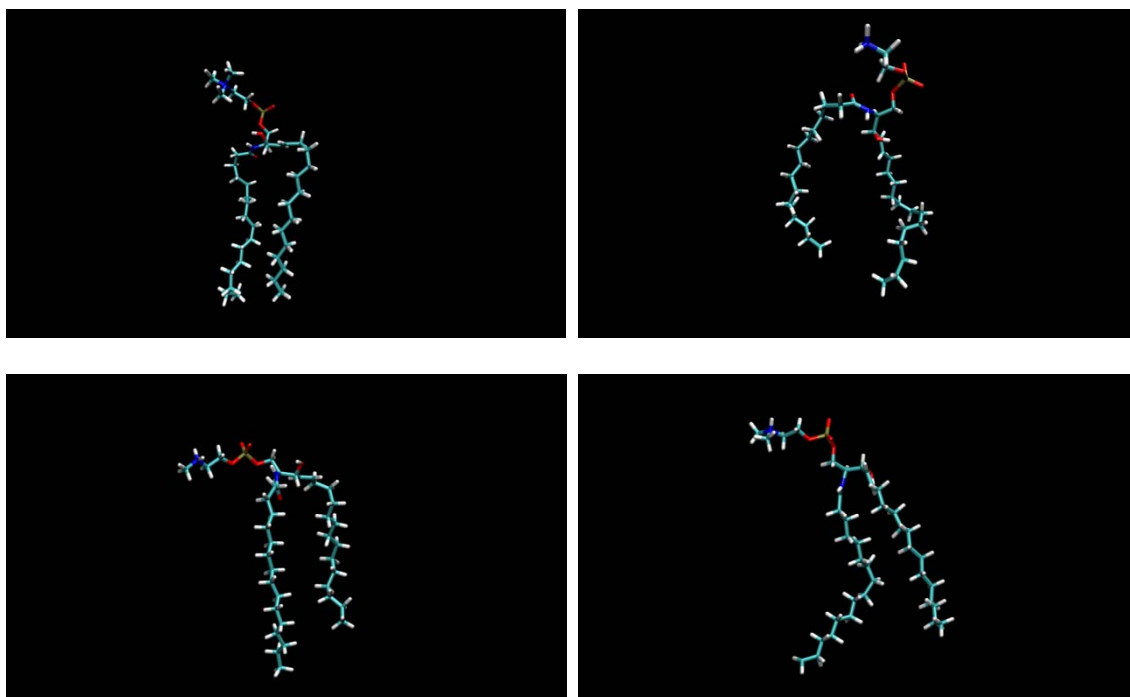


Figure S6. Snapshots of a selected PSM (*top left*), CPE (*top right*), CPE-Me (*lower left*), and CPE-Me₂ (*lower right*) molecule. One should keep in mind that the shown structures only illustrate the tendency of the N-H and N-C bonds' orientations, that is, they are not representative for all the molecules in the bilayer. For a view of the bond orientation, consider Figure 5 which shows a broad distribution of the angles between these bonds and the bilayer normal.



References

1. Yamamoto, T., H. Hasegawa, T. Hakogi, and S. Katsumura. 2006. Versatile synthetic method for sphingolipids and functionalized sphingosine derivatives via olefin cross metathesis. *Org. Lett.* 8:5569-5572
2. Fischer, R. T., F. A. Stephenson, A. Shafiee, and F. Schroeder. 1984. delta 5,7,9(11)-Cholestatrien-3 beta-ol: a fluorescent cholesterol analogue. *Chem. Phys. Lipids* 36:1-14
3. Bjorkbom, A., T. Yamamoto, S. Kaji, S. Harada, S. Katsumura et al. 2008. Importance of the phosphocholine linkage on sphingomyelin molecular properties and interactions with cholesterol; a study with phosphate oxygen modified sphingomyelin-analogues. *Biochim. Biophys. Acta* 1778:1501-1507
4. Bjorkbom, A., B. Ramstedt, and J. P. Slotte. 2007. Phosphatidylcholine and sphingomyelin containing an elaidoyl fatty acid can form cholesterol-rich lateral domains in bilayer membranes. *Biochim. Biophys. Acta* 1768:1839-1847
5. Bjorkqvist, Y. J., T. K. Nyholm, J. P. Slotte, and B. Ramstedt. 2005. Domain formation and stability in complex lipid bilayers as reported by cholestatrienol. *Biophys. J.* 88:4054-4063
6. Lakowicz, J. R. 2006. Principles of fluorescence spectroscopy. Springer Science+Business Media, LLC, New York.
7. Nyholm, T. K., P. M. Grandell, B. Westerlund, and J. P. Slotte. 2010. Sterol affinity for bilayer membranes is affected by their ceramide content and the ceramide chain length. *Biochim. Biophys. Acta* 1798:1008-1013
8. Lindahl, E., B. Hess, and D. van der Spoel. 2001. GROMACS 3.0: a package for molecular simulation and trajectory analysis. *Journal of Molecular Modeling* 7:306-317
9. van der Spoel, D., E. Lindahl, B. Hess, G. Groenhof, A. E. Mark et al. 2005. GROMACS: fast, flexible, and free. *J. Comput. Chem.* 26:1701-1718
10. Falck, E., M. Patra, M. Karttunen, M. T. Hyvonen, and I. Vattulainen. 2004. Lessons of slicing membranes: interplay of packing, free area, and lateral diffusion in phospholipid/cholesterol bilayers. *Biophys. J.* 87:1076-1091
11. Jorgensen, W. L., and J. Tirado-Rives. 1988. The OPLS [optimized potentials for liquid simulations] potential functions for proteins, energy minimizations for crystals of cyclic peptides and crambin. *Journal of the American Chemical Society* 110:1657-1666
12. Takaoka, Y., M. Pasenkiewicz-Gierula, H. Miyagawa, K. Kitamura, Y. Tamura et al. 2000. Molecular dynamics generation of nonarbitrary membrane models reveals lipid orientational correlations. *Biophys. J.* 79:3118-3138

13. Bayly, C. I., P. Cieplak, W. Cornell, and P. A. Kollman. 1993. A well-behaved electrostatic potential based method using charge restraints for deriving atomic charges: the RESP model. *The Journal of Physical Chemistry* 97:10269-10280
14. Frisch, M. J., G. W. Trucks, H. B. Schlegel, G. E. Scuseria, M. A. Robb et al. 2003. Gaussian 03, Revision C.02.
15. Jorgensen, W. L., J. Chandrasekhar, J. D. Madura, R. W. Impey, and M. L. Klein. 1983. Comparison of simple potential functions for simulating liquid water. *The Journal of Chemical Physics* 79:926-935
16. Rog, T., I. Vattulainen, and M. Karttunen. 2005. Modeling glycolipids: take one. *Cell Mol. Biol. Lett.* 10:625-630
17. Rog, T., I. Vattulainen, A. Bunker, and M. Karttunen. 2007. Glycolipid membranes through atomistic simulations: effect of glucose and galactose head groups on lipid bilayer properties. *J. Phys. Chem. B* 111:10146-10154
18. Hess, B., H. Bekker, H. J. Berendsen, and J. G. E. M. Fraaije. 1997. LINCS: A linear constraint solver for molecular simulations. *Journal of Computational Chemistry* 18:1463-1472
19. Parrinello, M., and A. Rahman. 1981. Polymorphic transitions in single crystals: A new molecular dynamics method. *Journal of Applied Physics* 52:7182-7190
20. Nose, S. 1984. A unified formulation of the constant temperature molecular dynamics methods. *The Journal of Chemical Physics* 81:511-519
21. Hoover, W. G. 1985. Canonical dynamics: Equilibrium phase-space distributions. *Phys. Rev. A* 31:1695
22. Essmann, U., L. Perera, M. L. Berkowitz, T. Darden, H. Lee et al. 1995. A smooth particle mesh Ewald method. *The Journal of Chemical Physics* 103:8577-8593
23. Rog, T., M. Pasenkiewicz-Gierula, I. Vattulainen, and M. Karttunen. 2009. Ordering effects of cholesterol and its analogues. *Biochim. Biophys. Acta* 1788:97-121
24. Hyslop, P. A., B. Morel, and R. D. Sauerheber. 1990. Organization and interaction of cholesterol and phosphatidylcholine in model bilayer membranes. *Biochemistry* 29:1025-1038
25. Davis, J. H. 1983. The description of membrane lipid conformation, order and dynamics by ²H-NMR. *Biochim. Biophys. Acta* 737:117-171
26. Pasenkiewicz-Gierula, M., Y. Takaoka, H. Miyagawa, K. Kitamura, and A. Kusumi. 1999. Charge pairing of headgroups in phosphatidylcholine membranes: A molecular dynamics simulation study. *Biophys. J.* 76:1228-1240
27. Murzyn, K., T. Rog, G. Jezierski, Y. Takaoka, and M. Pasenkiewicz-Gierula. 2001. Effects of phospholipid unsaturation on the membrane/water interface: a molecular simulation study. *Biophys. J.* 81:170-183

28. Pasenkiewicz-Gierula, M., T. Rog, K. Kitamura, and A. Kusumi. 2000. Cholesterol effects on the phosphatidylcholine bilayer polar region: a molecular simulation study. *Biophys. J.* 78:1376-1389
29. Pasenkiewicz-Gierula, M., Y. Takaoka, H. Miyagawa, K. Kitamura, and A. Kusumi. 1997. Hydrogen Bonding of Water to Phosphatidylcholine in the Membrane As Studied by a Molecular Dynamics Simulation: Location, Geometry, and Lipid Lipid Bridging via Hydrogen-Bonded Water. *The Journal of Physical Chemistry A* 101:3677-3691